EUROPEAN CONFERENCE ON INTEGRATED OPTICS

# Multiphysics simulation approach for polymer waveguide microring resonator based ultrasonic detectors

**Jan-Jonas Schumacher[1], Paul Muellner[1], Moritz Eggeling[1], Rainer Hainberger[1]**

[1]AIT Austrian Institute of Technology GmbH, Giefinggasse 4, Vienna, 1210, Austria
* rainer.hainberger@ait.ac.at

**We report a 2D FEM simulation approach to analyse the dynamic structural and optical response of polymer waveguides to ultrasonic waves in dependence of material parameters, acoustic frequency, and angle of incidence. This simulation approach provides better physical insight and facilitates the optimization of microring resonator based ultrasonic detectors.**
***Keywords***: *polymer mircoring resonator, multiphysics simulation, ultrasonic detection*

## INTRODUCTION

Polymer microring resonators (MRR) have proven to be very attractive ultrasonic detectors due to their high sensitivity, large frequency range, and compactness [1,2]. Despite successful experimental use for photoacoustic imaging over many years, thorough multiphysics simulations of the ultrasonic detection mechanisms considering the frequency and angle dependent response of the waveguide structure have not yet been reported. In this study, we take a major step in this direction by introducing a suitable simulation approach.

Figure 1a) illustrates the operation principle of an MRR-based ultrasonic detector. Here, we assume a spherical ultrasound wave being generated by an acoustic point source in water with amplitude $A$ and frequency $f$, where the pressure at a distance $R$ can be expressed as $u(R,t) = A/R\, e^{i2\pi f(t-R/c_s)}$ with $c_s$ being the speed of sound in water. Without incident ultrasonic wave the condition for the $m$-th order resonance in an MRR with radius $r$ is given by

$$m\lambda_m = n_{\mathrm{eff},0}\, 2\pi r, \tag{1}$$

where $\lambda$ the wavelength and $n_{\mathrm{eff},0}$ the unperturbed effective refractive index of the guided optical mode. The ultrasonic wave induces changes of the local effective refractive index along the MRR. The change of the local effective refractive index at a specific position on the MRR at the point of time $t$, depends on the local pressure $u(R,t)$, the direction of incidence $\vec{R}/|\vec{R}|$, and the frequency of the ultrasonic wave. Therefore, the time dependent resonance condition of an MRR perturbed by the incident ultrasonic spherical wave can be written as

$$m\lambda_m(t) = \int_0^{2\pi} n_{\mathrm{eff}}\big(\varphi, f, \Phi(t)\big) r d\varphi, \tag{2}$$

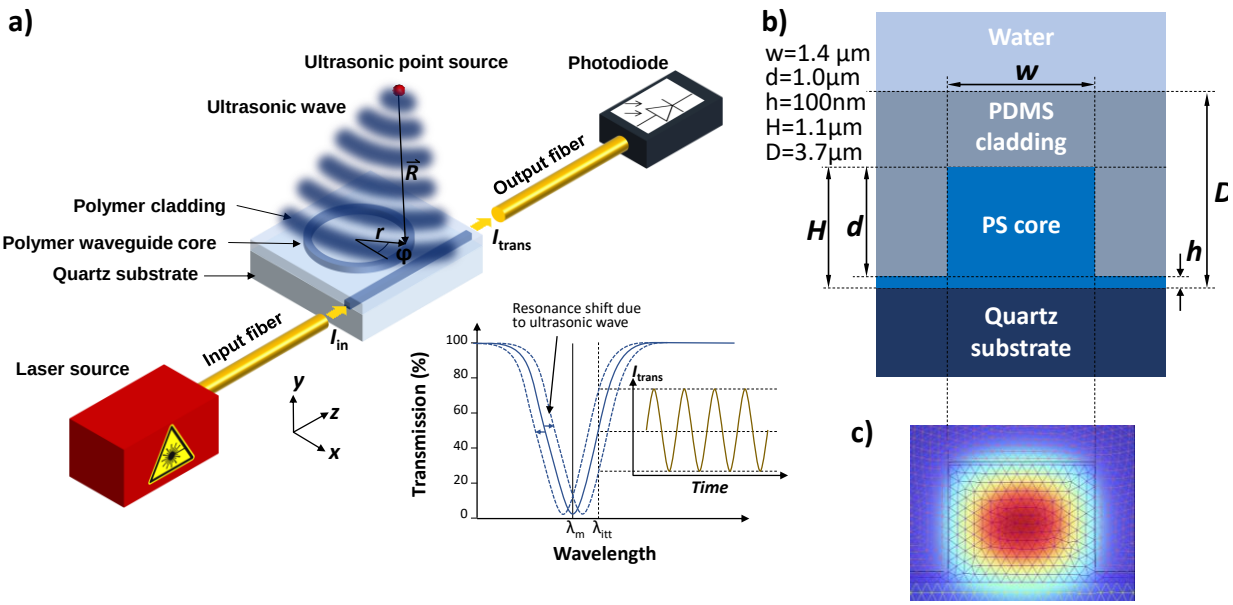


*Fig. 1. a) Operation principle of an MRR used as ultrasonic detector, where the shift of the optical resonance interrogated at $\lambda_{itt}$ results in a modulation of the transmitted optical power $I_{trans}$, b) waveguide cross-section, c) FEM eigenmode analysis of deformed waveguide structure.*

where the polar angle $\varphi$ is used to parametrize the position on the MRR and $\Phi(t) = t - R/c_s$ is the local phase value of the acoustic wave. The ultrasound wave exerts pressure on the waveguide structure, leading to deformation and stress in the structure. The deformation of the waveguide core cross section modifies the effective refractive index. In addition, the stress $\sigma$ in the core and cladding material directly changes the local refractive index due to the elasto-optic effect, which can be defined as [3]:

$$n_x \approx n_0 - C_1\sigma_x - C_2(\sigma_y + \sigma_z) \quad (3a)$$

$$n_y \approx n_0 - C_1\sigma_y - C_2(\sigma_x + \sigma_z) \quad (3b)$$

$$n_z \approx n_0 - C_1\sigma_z - C_2(\sigma_x + \sigma_y) \quad (3c)$$

In the equations above (3a-c), $n_x$, $n_y$, and $n_z$ are the refractive indices for light polarized in the *x*-, *y*-, and *z*-direction. $n_0$ is the refractive index of the material without stress and $C_1$ and $C_2$ are the elasto-optic constants. The stress components are denoted by $\sigma$, where the subscript defines the stress direction.

We employed COMSOL for a 2D Finite Element Method (FEM) based multiphysics study of the structural and optical response of the polymer waveguide shown in Figure 1b) to an incident ultrasonic wave in water. We assumed that the acoustic wavefront can locally be represented as plane wave. Table 1 summarizes the physical parameters used in the simulations. In a first step, the deformation of the waveguide structure in response to the acoustic wave was calculated. The bottom of the glass substrate was positioned by a fixed constraint, assuming negligible displacements of the glass. Since we consider fabrication by nanoimprint lithography, we include a residual layer next to the waveguide core of 100 nm thickness. We added an isotropic loss factor damping value η=0.01 for the PDMS cladding, which is a typical value for rubber-like materials [4]. In a second step, an optical eigenmode analysis for the deformed structure was performed (see Figure 1c)) considering the deformation and the elasto-optic effect due to strain. The optical wavelength λ in our simulations was set to 780 nm. We could not find experimental data for $C_1$ and $C_2$ of PDMS in literature. However, birefringence measurements for transparent rubbers suggest a relative elasto-optic constant $C_0 = C_2 - C_1$ beyond 1000 TPa$^{-1}$ [5,6]. Therefore, we exemplarily investigated two combinations of $C_1$ and $C_2$ with a fixed relative elasto-optic constant $C_0$= 2000 TPa$^{-1}$. The deformation of the coupling region is neglected [1]. A change in the ring radius is also considered to be insignificant due to the assumption of a stiff substrate and strong adhesion of the polymer core material to the glass.

| Material | Young's modulus (MPa) | Poisson's ratio | Density (kg/m$^3$) | $n_0$ | $C_1$ (TPa$^{-1}$) | $C_2$ (TPa$^{-1}$) |
|---|---|---|---|---|---|---|
| Polystyrene (PS) | 300 | 0.33 | 965 | 1.5775 | 48* | 29* |
| Polydimethylsiloxane (PDMS) | 0.75 / 1.5 / 3.0 | 0.49 | 1000 | 1.4050 | 0<br>1000 | 2000<br>3000 |
| Glass | 7250 | 0.17 | 2210 | 1.4540 | | |

*Table 1: Physical constants used in simulation (*elasto-optic constants from [7] at 632.8 nm).*

**RESULTS AND DISCUSSION**

Figures 2a)-c) show the change of the effective refractive index $n_{\mathrm{eff}}$ of the TM-like guided mode in the waveguide under the influence of an ultrasonic wave with the local pressure amplitude on the surface of the cladding of 0.1 MPa as a function of the phase of the acoustic wave for three different frequencies (1 MHz, 10 MHz, 100 MHz) and two angles of incidence (0° and 20° with respect to the surface normal). The blue curves show the change purely caused by the geometric deformation of the waveguide core, *i.e.*, without considering the elasto-optic effect. Positive strain values compress the waveguide core, resulting in a reduced $n_{\mathrm{eff}}$. On the other hand, the elasto-optic effect increases the refractive material index for positive strain values [1]. Therefore, these two phenomena have a counteracting effect on $n_{\mathrm{eff}}$ as can be seen in the orange curves in Fig. 2, which include the elasto-optic effect. For 100 MHz, the PDMS cladding material (Young's modulus $E_{\mathrm{PDMS}}$=0.75 MPa) cannot follow the ultrasonic wave any more instantaneously and there is a phase lag between the structural oscillation of the waveguide and the sound wave. Next, we investigated the influence of the pressure on the effective refractive index change $\Delta n_{\mathrm{eff}}$ over a full period of the acoustic wave (Fig. 3a). Figure 3b summarizes the slope values $d\Delta n_{\mathrm{eff}}/dP$ for the different PDMS elasto-optic constants and angles of incidence using $E_{\mathrm{PDMS}}$=0.75 MPa. The sensitivity of the refractive index change to the pressure clearly reduces with increasing frequency. In Fig 3c), also different values for $E_{\mathrm{PDMS}}$ are investigated. Higher values of $E_{\mathrm{PDMS}}$ result stronger optical response assuming that the elasto-optic constants of PDMS do not change.

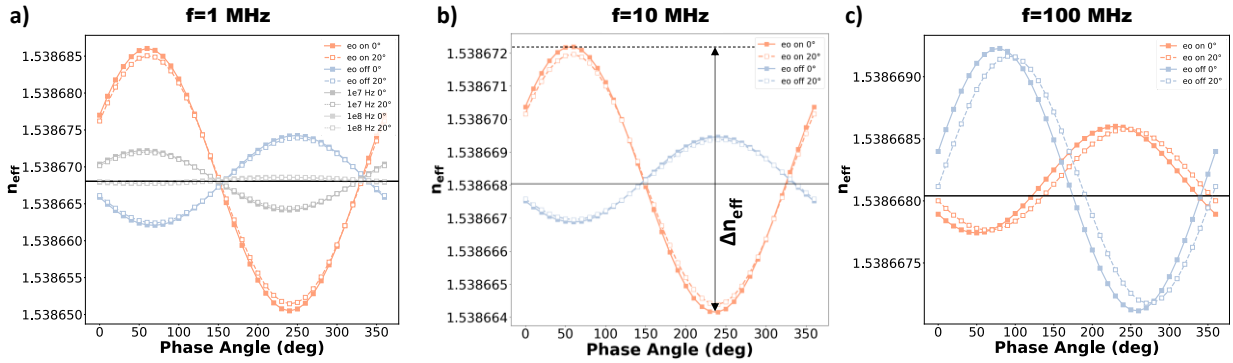


*Fig. 2. Change of the effective refreactive index $n_{eff}$ for different phase angles of the incident acoustic wave (0.1 MPa) without (eo off, blue lines), i.e. only geometric deformation, and with taking into account the elasto-optic effect (eo on, orange lines) for incident angles of 0° and 20°. The black line indicates the mode index of the non-deformed waveguide. For PDMS, a Young's modulus of 0.75 MPa and elasto-optic constants $C_1$=1000 $TPa^{-1}$ and $C_2$=3000 $TPa^{-1}$ were assumed. a) Ultrasound frequency 1 MHz with added 10 MHz and 100 MHz(both only with elasto-optic effect) to display the amplitude scaling, b) 10 MHz, c) 100 MHz.*

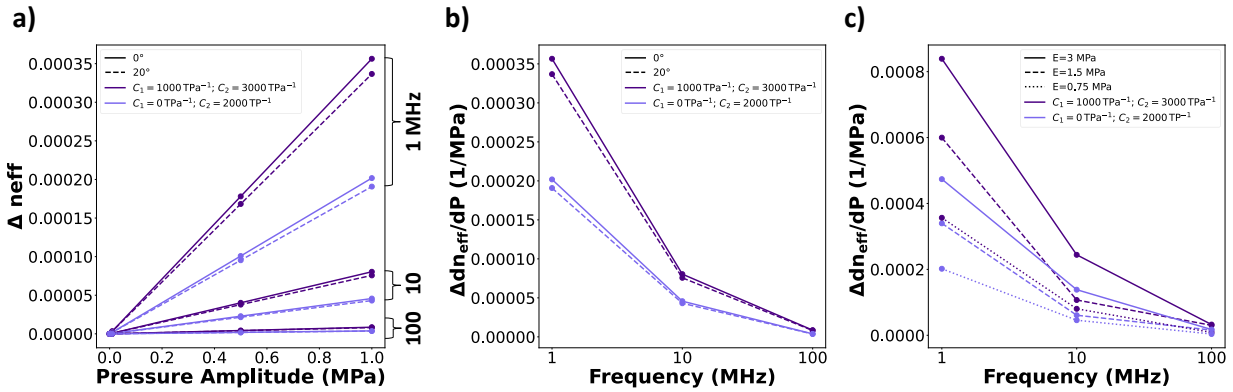


*Fig. 3. a) Effective refractive index change $\Delta n_{eff}$ over a full period of the acoutic wave as a function of the pressure amplitude ($E_{PDMS}$ = 0.75 MPa, b) Slope $d\Delta n_{eff}/dP$ ($MPa^{-1}$) as function of frequency for two different elasto-optic constant settings for PDMS and two angles of incidence using $E_{PDMS}$ = 0.75 MPa, c) Slope $\Delta n_{eff}/\Delta P$ ($MPa^{-1}$) as funtion of frequency for three different values of $E_{PDMS}$ and an angle of incidence 0°.*

## CONCLUSION AND OUTLOOK

In this work, we have proposed a 2D FEM simulation model to analyse the dynamic structural and optical response of polymer waveguides to ultrasonic waves in dependence of material parameters, acoustic frequency, and angle of incidence. As a next step, we will use the model to generate data for calculating the wavelength shift of the MRR according to equation (2), which allows for a 3D approximation in a generalized form of the approach reported in [8].

Acknowledgements: This work was supported by the REAP project, which received funding from the European Union's Horizon 2020 research and innovation programme under grant agreement No 101016964 under the Photonics Public Private Partnership (PPP) call H2020-ICT-2020-2 with the topic ICT-36-2020 - Disruptive photonics technologies.

## References

[1] C.-Y. Chao et al., *High-frequency ultrasound sensors using polymer microring resonators*, IEEE Transactions on Ultrasonics, Ferroelectrics, and Frequency Control, vol. 54, no. 5, pp. 957–965, 2007

[2] S. Ashkenazi et al., *Ultrasound detection using polymer microring optical resonator*, Applied Physics Letter, vol. 85, no. 22, pp. 5418–5420, 2004

[3] D. L. MacAdam et al., *Matrix Theory of Photoelasticity*, Springer, Berlin Heidelberg, 1979

[4] COMSOL Multiohysics, *Damping in Structural Dynamics: Theory and Sources*, https://www.comsol.de/blogs/damping-in-structural-dynamics-theory-and-sources/ (accessed: Jan. 31 2023), Stockholm

[5] A. Angioletti et al., *Rubber Birefringence and Photoelasticity*, Rubber Chemistry and Technology, vol. 38, no. 5, pp. 1115–1163, 1965

[6] Y. Hazan et al., *Silicon-photonics acoustic detector for optoacoustic micro-tomography*, Nature Communications, vol. 13, no. 1, p. 1488, 2022

[7] F. Ay et al., *Prism coupling technique investigation of elasto-optical properties of thin polymer films*, Journal of Applied Physics, vol. 96, no. 12, pp. 7147–7153, 2004

[8] Z. Zhang et al., *Theoretical and experimental studies of distance dependent response of micro-ring resonator-based ultrasonic detectors for photoacoustic microscopy*, Journal of Applied Physics 116 (14), p. 144501, 2014